Front. Earth Sci. 2018, 12(3): 569–582
https://doi.org/10.1007/s11707-018-0677-0

RESEARCH ARTICLE

Assessment of trace metal contamination in groundwater in a highly urbanizing area of Shenfu New District, Northeast China

Yintao LU[1,2], Xinghua ZANG[1,2], Hong YAO (✉)[1,2], Shichao ZHANG[1,2], Shaobin SUN[1,2], Fang LIU[1,2]

1 School of Civil Engineering and Architecture, Beijing Jiaotong University, Beijing 100044, China
2 Beijing Key Laboratory of Aqueous Typical Pollutants Control and Water Quality Safeguard, Beijing 100044, China

Abstract Shenfu New District, located between two old industrial cities, Shenyang and Fushun, is a typical area undergoing industrialization and urbanization in China. The sources and distributions of heavy metals were analyzed in groundwater by multivariate analysis and GIS, and the impact of urbanization on the aqueous distribution of these metals was investigated. The results indicated that the mean contents of zinc (Zn), arsenic (As), cadmium (Cd), and lead (Pb) in the wet periods were about two times of those in the dry period. Nickel (Ni) and chromium (Cr) were considered to be associated with the same anthropogenic origins (i.e., wastewater from agricultural processing). The concentration of Zn was high under natural conditions, but was also affected by human activities (e.g., wastewater from foundry and instrument manufacturers). As, Cd, and Pb are likely derived from both anthropogenic and natural sources (agricultural and water-rock interactions). The spatial distributions of heavy metals in groundwater were region-specific, with the highest concentrations mostly along the Hun River. The heavy metal pollution index (HPI) values from the dry and wet periods showed similar trends at different sampling sites. Only one site's HPI was above the critical value of 100. These results provide information that can be used to understand potential threats to the groundwater resources of other developing cities.

Keywords heavy metals, groundwater pollution, hydrochemical type, spatial distribution, seasonal variation, risk assessment

Received May 11, 2016; accepted August 27, 2017

E-mail: yaohongts@163.com

1 Introduction

Water pollution is a major public health concern worldwide (Erbahar et al., 2016; Strugała-Wilczek and Stańczyk, 2016). Water quality is strongly influenced by intense industrial activities and urbanization, which is the result of increasing population density in urban areas that adversely affect aquatic systems (De Nicola et al., 2015; Xu et al., 2015; Zhang et al., 2015a). Heavy metals are the most common persistent toxic contaminants during urbanization (Borrell et al., 2016; Peng et al., 2016). Accordingly, an analysis of the heavy metal content in groundwater is imperative to understand their sources, fates, and potential health risks. A number of studies have indicated that heavy metals entering an aquatic environment may be from anthropogenic or natural sources (Baumann et al., 2006; Cui and Shi, 2012). The major natural sources are petrochemical and volcanic activities, and geochemical weathering (Wuana and Okieimen, 2011). Anthropogenic sources include effluents from the seepage of oil wells, tankers, and other oil extraction activities, oil spillage on crop farms, mining extractions, transportation, and related activities (Nwaichi et al., 2014).

With the initiation of the New Silk Road, the Chinese government introduced more human activities to nearly all regions of China and mid-Asia (Li et al., 2015). With the implementation of some major projects in recent years, China's economy developed rapidly (Li et al., 2017) in concert with high-speed urbanization, putting potential pressure on water quality (Li et al., 2015). In accordance with the urban and rural planning announced by the government of Shenfu New District, while the proportion of urban land use in 2010 was only 5%, the proportion in 2020 will reach 43%. In addition, while the population of Shenfu New District in 2015 was similar to that in 2014, approximately 257,000 villagers vacated over that time,

indicating that the rural population is rapidly moving to the city. As a result, the groundwater in the area has suffered from a number of human-induced changes, including reclamation/farming, industrial production, urbanization, and mining (Guo et al., 2010; Sun et al., 2011; Yao et al., 2012). The groundwater is also susceptible to pollution from natural processes, such as leaching, precipitation, and infiltration (Wang et al., 2010; Guo and He, 2013; Zhang et al., 2013; Wang et al., 2015), resulting in soil erosion and a reduction in water quality and aquatic biodiversity.

The distribution of heavy metals in groundwater has been studied throughout the world, especially in areas affected by urban growth (Dokou et al., 2015; Mehrabi et al., 2015; Kujawska et al., 2016). Since groundwater varies widely with climatic and geochemical conditions (Hosseinifard and Aminiyan, 2015; Al-Omran et al., 2016; Long et al., 2016), a proper understanding of groundwater pollution caused by urbanization is pertinent. Studies have shown that heavy metals in the groundwater are directly related to natural and anthropogenic disturbances (Hosseinifard and Aminiyan, 2015; Siegel et al., 2015; Rasool et al., 2016). In spite of intensive research, there is little information on the seasonal variation of heavy metals in groundwater (wet periods vs. dry periods).

The present study investigated chromium (Cr), nickel (Ni), zinc (Zn), arsenic (As), cadmium (Cd), and lead (Pb) concentrations in groundwater in an urbanizing area in the Shenfu New District. The aims of this study were to: 1) investigate the distribution patterns of heavy metals and determine their hydrochemical characteristics in groundwater, 2) determine the possible sources of heavy metals in groundwater and seasonal variations, and 3) assess the potential harm to public health and obtain data for comparison with other areas. The results provide information that can be used to understand potential threats to the groundwater resources of other developing cities.

2 Materials and methods

2.1 Study area and sampling

The study area (41°39′N–42°3′N, 123°33′E–123°57′E) is located between Shenyang and Fushun and covers approximately 605 km^2. The Hun River flows through the area from east to west (Fig. 1). This region has an annual mean temperature between 4°C and 8°C and is subject to the temperate continental monsoon climate. The average annual precipitation is 800 mm, with 70%–80% of the rainfall observed from June to August (Zhang et al., 2009). The Hun River provides a considerable amount of water for agricultural, domestic, industrial, and other purposes.

The lithology of the upper geologic formation is mainly Quaternary alluvial deposits whereas the lithology of the lower geologic formation is primarily Tertiary lacustrine deposits. The eastern mountains of the study area comprise the main groundwater recharge area. Water from precipitation and leakage infiltration from the Hun Riverbed recharges the nearby groundwater (Peng et al., 2015). The groundwater primarily flows northeast to southwest. Artificial exploitation is the main groundwater form of discharge (Gao et al., 2015). The groundwater in the study area can be sectioned into three local aquifer systems: 1) a

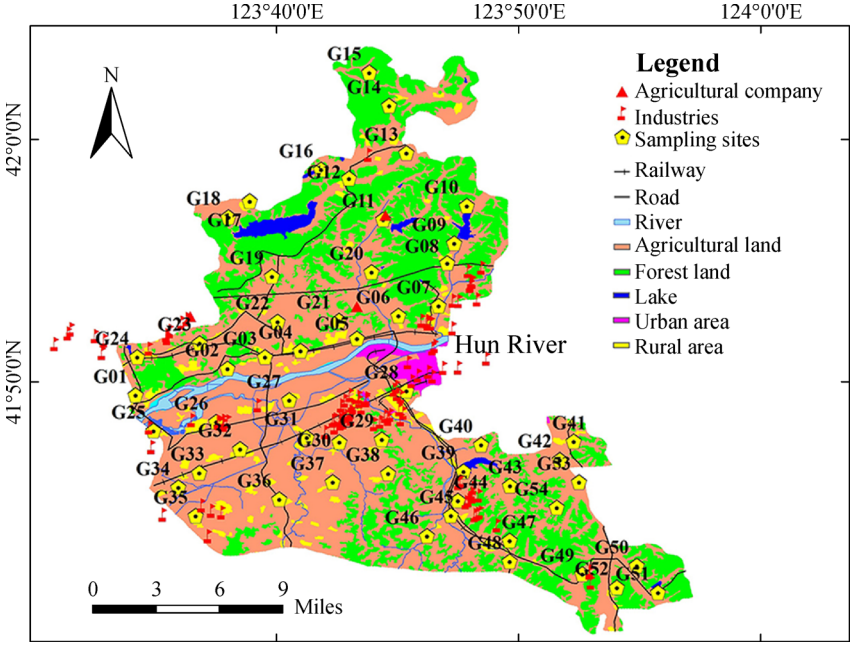

Fig. 1 Sampling site locations.

Holocene alluvial layer, composed of grit, hosts phreatic water, with a groundwater depth of 5–22 m; 2) an upper Pleistocene alluvial-diluvial layer, composed of grit and gravel, holds confined water at a depth of 8–30 m under the north bank of the Hun River and 3–9 m under the south bank; and 3) a middle Pleistocene layer, composed of outwash gravel sand and circular-gravel, has confined pore water (Fig. 2) at a depth of 15–50 m located in the lowest part of the Quaternary strata (Cui et al., 2014; Su et al., 2015). The basement rocks include shale, sandstone, limestone, granite, calcite, and gneiss (Su et al., 2015). The predominant land use type in this area is non-urban, such as agricultural and forest land (Fig. 1).

Agricultural product processing factories, petroleum and chemical companies, foundries, and manufactories are mainly distributed in areas near the river. Land use has increasingly been converted from non-urban to urban, evidenced by rapid economic development and a rise in building construction. A consequence has been a serious deterioration of the aquatic environment in the area.

Fifty-four ground water samples were collected during the dry period of December 2014 and the wet period of July 2015. Samples were collected from the wells of local residents, which have been open for public use. The distribution of the ground water sampling points is shown in Fig. 1. The 0.01°×0.01° grid file of study area was generated with ARCGIS10.0. Every grid central point was set as a survey point.

2.2 Analytical methods

Groundwater samples were collected from 5–100 m below the ground surface. The water pumped to the surface during the initial 5–10 min was discarded; subsequent samples were collected in thoroughly rinsed polyethylene bottles. Parameters including pH, oxidation reduction potential (ORP), electrical conductivity (EC), and salinity (SAL) were determined in the field. The pH and ORP were determined using a Hach Portable pH/ORP Meter (HQ11d). The EC and SAL were determined using a Hach conductivity meter (HQ14d). The instruments were calibrated before each sample was determined. For metal analyses, water samples were filtered through a 0.45 μm filter. The samples were then acidified *in situ* to a pH of less than 2 with ultrapure HNO_3. All water samples were kept in sealed containers at 4°C prior to analysis. The concentrations of As, Pb, Cr, Ni, Cd, and Zn were analyzed by inductively coupled plasma spectrometry-mass spectrometry (ICP-MS, Agilent Technologies 7500a, USA). The concentrations of Ca, K, Na, and Mg were measured by a Perkin Elmer model Optima instrument. The limit of detection for the investigated metals was 0.1 $\mu g \cdot L^{-1}$ for Pb, 0.5 $\mu g \cdot L^{-1}$ for As and Zn, 0.2 $\mu g \cdot L^{-1}$ for Ni, 0.001 $mg \cdot L^{-1}$ for Cr, 0.1 $\mu g \cdot L^{-1}$ for Pb, and 0.05 $mg \cdot L^{-1}$ for Ca, Na, K, and Mg. Water samples were left unacidified and unfiltered for anion analyses. The concentrations of Cl^- and SO_4^{2-} were determined using

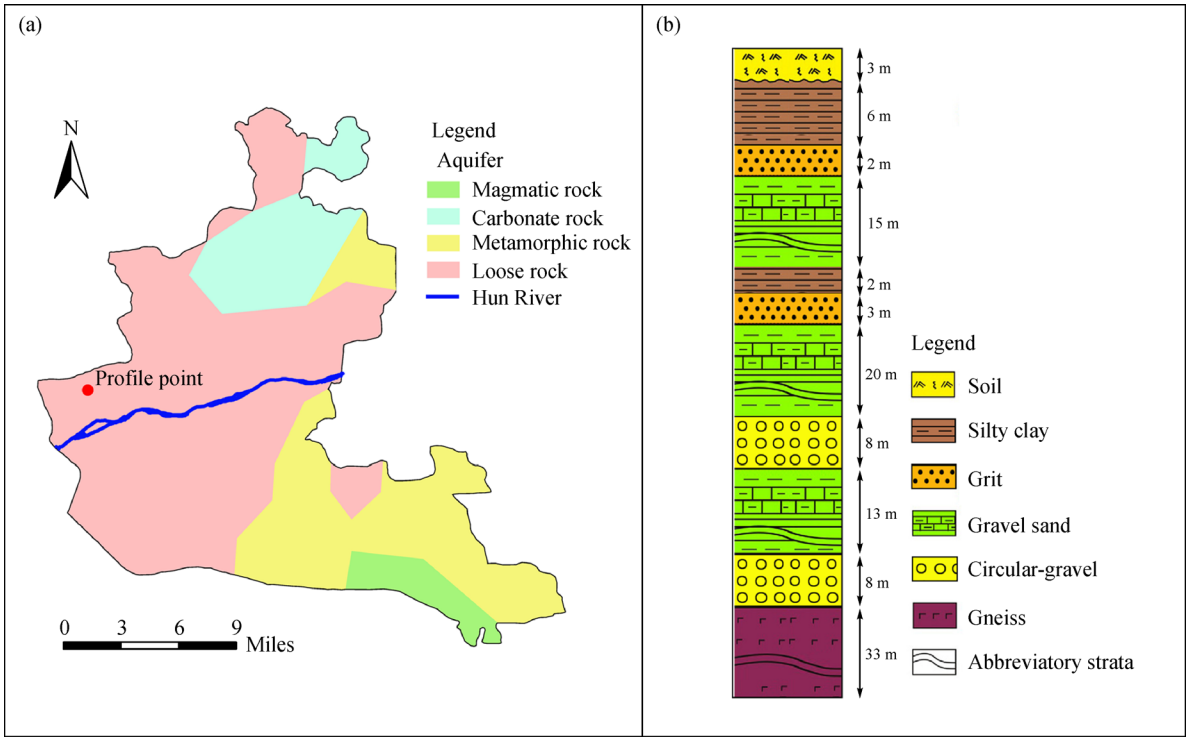

Fig. 2 Aquifer information and sediment profile in the study area. (a) The aquifer in the mountainous region in the north contains carbonate rock, composed of limestone and calcite. (b) Sediment profile of the profile point.

ion chromatography (Shimadzu CTO-10A), and the concentration of HCO_3^- was determined by titration. The precision for the anions and cations was verified by ionic balance error. The errors were in the range of ±5%. Sample batches were regularly interspersed with blanks and standards. All data were corrected for instrument drift and a five-point calibration curve was constructed for each element. The National Institute of Standards values of China were used to check the reliability of the analyses.

2.3 Pollution assessment indices

The heavy metal pollution index (HPI) method provides the total level of heavy metals in drinking water (Prasad and Sangita, 2008). The method was established by assigning weightage (W_i) for each heavy metal. The weightage is a value in the range between zero and one. This value can be defined as inversely proportional to the recommended standard (S_i) for each metal (Prasad and Jaiprakas, 1999). The permissible value (S_i) and desirable value (I_i) were taken from the drinking groundwater standards of the US Environmental Protection Agency (USEPA), the Pollution Control Department of Thailand (PCD), the World Health Organization (WHO), and regional (China) drinking water specifications (Standards for Drinking Water Quality (GB5749-2006)) for this study. The highest S_i refers to the maximum allowable concentration in drinking water. The maximum I_i indicates the standard limits for the same heavy metals in drinking water.

The HPI was determined by the following equation (Prasad and Jaiprakas, 1999):

$$\mathrm{HPI} = \frac{\sum_{i=1}^{n} W_i Q_i}{\sum_{i=1}^{n} W_i}, \quad (1)$$

where W_i is the unit weight of the (i) parameter, Q_i is the sub-index of the (i) parameter, and n is the number of considered parameters. The sub index (Q_i) of the parameter was calculated with the following equation:

$$Q_i = \sum_{i=1}^{n} \frac{|M_i - I_i|}{S_i - I_i} \times 100, \quad (2)$$

where M_i, S_i, and I_i are the monitored heavy metal, standard, and ideal values of the (i) parameter, respectively. Generally, the critical pollution index value is 100.

2.4 Multivariate statistical and spatial analysis

Correlation analysis and hierarchical cluster analysis were used to identify clusters of metals and their inter-element relationships, which also provided noteworthy information on metal element sources (Rodríguez et al., 2008; Wu et al., 2014). SPSS version 22 for Windows (SPSS Inc., Chicago, IL, USA) and Microsoft Excel, 2010 (Microsoft, 2010) were used for all statistical analyses. Geostatistical methods are common approaches to characterize the spatial distribution of contaminant concentrations in groundwater and soil (Zou et al., 2015). The basic principle is to make an unbiased estimate for the values of sampled locations by considering their spatial correlation with the sampled points and minimizing the variance in the estimation error. Ordinary kriging (OK), the most robust and common interpolation method, was used. ArcGIS version 10.2 (ESRI Inc., Redlands, CA, USA) was used for mappings.

3 Results and discussion

3.1 Physicochemical characteristics of groundwater

The hydrochemical characteristics of groundwater are summarized in Table 1. Electrical conductivities varied from 39.50 μS/cm to 537.00 μS/cm with a mean of 286.34 μS/cm in the dry period and from 48.60 μS/cm to 342.00 μS/cm with a mean of 161.55 μS/cm in the wet period in Shenfu New District; all were below the recommended values (1500 μS/cm) set by WHO. The groundwater samples were slightly acidic to slightly alkaline with pH from 6.02 to 7.11 in the dry and 6.37 to 8.77 in the wet period, with the presence of carbonate minerals preventing the formation of acidic water in the area (except G13 and G28).

The mean concentrations of K^+, Ca^{2+}, Na^+, and Mg^{2+} in groundwater in the dry period were (2.99, 66.51, 22.31, and 21.12) $mg \cdot L^{-1}$, and (2.48, 45.63, 16.38, and 15.54) $mg \cdot L^{-1}$ in the wet period, respectively (Table 1). The concentrations of cations follow the order of $Ca^{2+} > Na^+ > Mg^{2+} > K^+$ in both periods. The mean concentrations of major anions Cl^-, SO_4^{2-} and HCO_3^- were (153.20, 211.09, and 287.69) $mg \cdot L^{-1}$ in the dry period, and (39.57, 61.24, and 211.21) $mg \cdot L^{-1}$ in the wet period, respectively. The concentrations of anions follow the order of $HCO_3^- > SO_4^{2-} > Cl^-$ in both dry and wet periods. However, the concentrations of Cl^-, SO_4^{2-}, HCO_3^-, and Ca^{2+} in the dry period were significantly higher than in the wet period.

To gain a better understanding of the role of water-rock interactions in aquifer, human activities, and groundwater evaporation in regulating groundwater chemistry, it is necessary to investigate the hydrogeochemical transition of groundwater (Li et al., 2016a). Plotting major anions and cations in a Piper diagram (Piper, 1944; Fig. 3) revealed Ca-Mg-HCO_3 and Ca-Mg-SO_4 water types in both wet and dry periods. The Ca-Mg-HCO_3 type is considered to be alkaline earth water, which very likely suggests weathering of carbonate minerals (calcite minerals and dolomite) (Wang and Jiao, 2012). The Ca-Mg-SO_4 type falls within the alkaline earth water and constituted approximately 50% of the samples in both dry and wet periods, indicating

Table 1 The concentration of some groundwater properties

Item	Dry period (n = 54)					Wet period (n = 54)				
	Min	Mean	Max	SD	CV	Min	Mean	Max	SD	CV
pH	6.02	6.96	7.71	0.42	6	6.37	7.09	8.77	0.37	5.3
EC/(μS·cm^{-1})	39.5	286.34	537	97.43	34	48.6	161.55	342	76.19	47.2
Salinity	70.8	137.81	255	44.33	32.2	23	76.42	164	36.36	47.58
ORP/(mV)	–55.10	*NA*	43.7	*NA*	*NA*	–73.10	*NA*	39.3	*NA*	*NA*
Cr/(μg·L^{-1})	8.52	11.64	21.15	2.23	19.2	4.73	7.03	14.24	1.88	26.68
Ni/(μg·L^{-1})	2.24	5.29	47.94	6.06	114.49	1.03	3.4	31.16	4.48	131.65
Zn/(μg·L^{-1})	0.71	12.28	98.35	21.76	177.14	2.65	35.44	607.4	101.54	286.51
As/(μg·L^{-1})	1.09	2.3	3.49	0.51	22.36	2.52	3.36	4.66	0.48	14.37
Cd/(μg·L^{-1})	0.17	0.61	0.84	0.08	13.49	1	1.01	1.07	0.01	1.24
Pb/(μg·L^{-1})	1.98	3.62	25.46	3.18	87.97	7.26	7.66	9.01	0.32	4.21
K/(mg·L^{-1})	0.75	2.99	15.65	2.73	91.46	0.32	2.48	19.81	4.57	184.25
Ca/(mg·L^{-1})	32.1	66.51	132.7	24.84	37.35	1.21	45.63	166.7	40.82	89.45
Na/(mg·L^{-1})	5.09	22.31	65.34	11.4	51.1	2.11	16.38	83.18	19.45	118.71
Mg/(mg·L^{-1})	7.47	21.12	50.84	8.84	41.84	3.02	15.54	47.36	12.84	82.59
Cl$^-$/(mg·L^{-1})	29	153.2	784.19	125.01	81.6	2.3	39.57	358.47	55.67	140.68
SO_4^{2-}/(mg·L^{-1})	31.09	211.09	682.77	122.02	57.8	5.04	61.24	450.61	63.57	103.8
HCO_3^-/(mg·L^{-1})	168.275	287.69	366.58	56.67	19.7	93.28	211.21	291.58	56.18	26.6

Remarks: ''SD'' represents standard deviation; ''CV'' (in %) represents coefficient of variation. *NA* = not available.

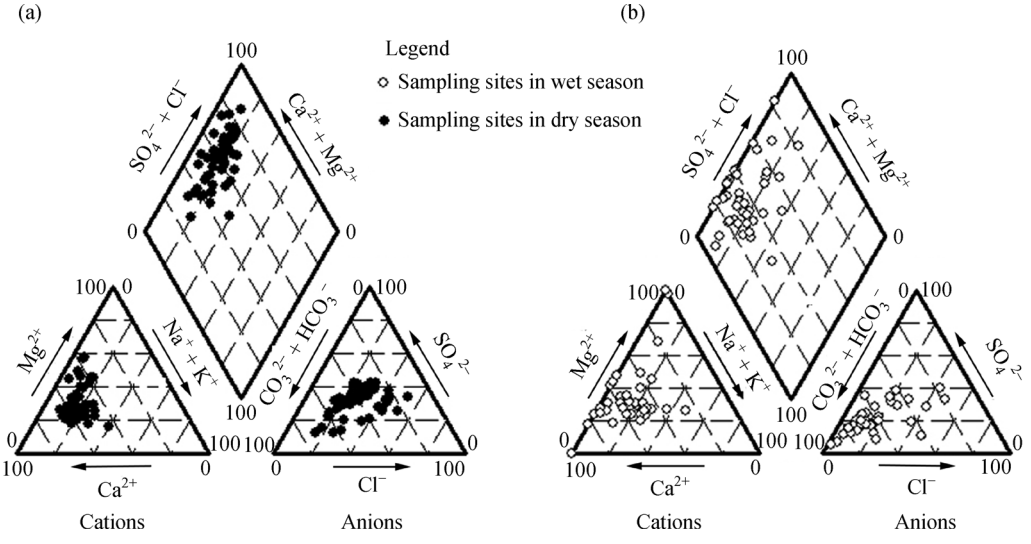

Fig. 3 Plot of major ions on a Piper diagram for dry and wet seasons. (a) Dry season; (b) wet season.

that the groundwater of these sites may have been formed via similar hydrochemical processes. Groundwater in the study area showed typical characteristics of recharge water of a regional groundwater system: enriched HCO_3^- and Ca^{2+}, low TDS, and slightly alkaline pH (Li et al., 2016b).

The plotting of groundwater samples in $Na^+/(Na^+ + Ca^{2+})$ versus the TDS diagram (Gibbs, 1970) shows that all groundwater samples fall in the rock weathering field (Fig. 4). This suggests that combinations of anions and cations in the area are controlled by the weathering and mineralogical characteristics of the bedrock and minerals, such as silicates and carbonates. Thus, mineral dissolution and weathering are the major processes that regulate groundwater chemistry in the study area. However, this does not necessarily mean that groundwater formation mechanisms are completely free from human interference (Li et al., 2016a). Indirect impacts, such as groundwater governance regulations, groundwater abstraction, and the

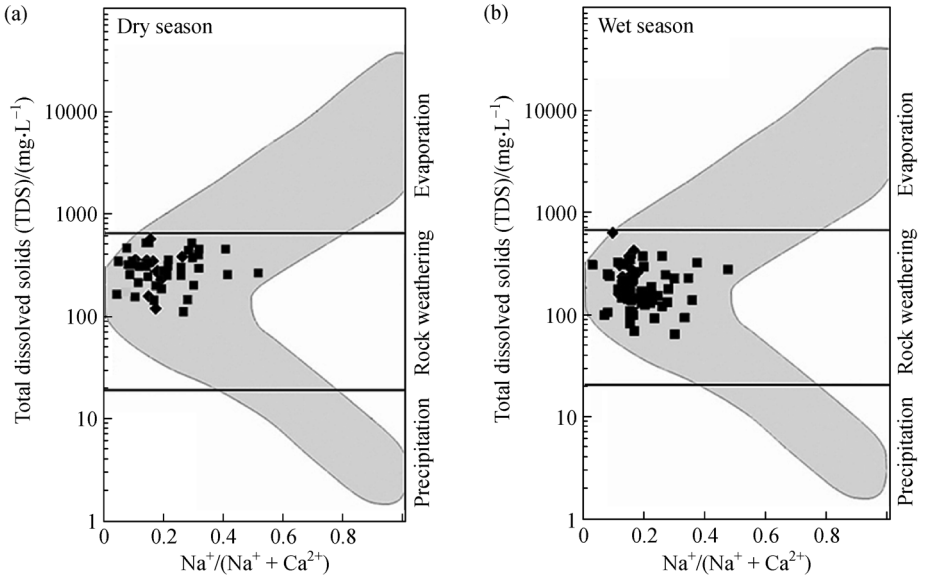

Fig. 4 Plot of total dissolved solids vs. relative cations for water in dry and wet seasons (Gibbs plot). (a) Dry season; (b) wet season.

groundwater management framework, do not alter the groundwater chemical compositions directly. They can, however, have an indirect influence by altering hydrodynamic conditions that may change groundwater evaporation intensity and accelerate water-rock interaction processes. This may illuminate the chemical evolution of groundwater based on the impact of human activities (Li et al., 2017). For example, the revival of the Silk Road economic belt, which is quite important in China and central Asian countries, can indirectly influence groundwater quality and development (Li et al., 2015). The increase in human activity has resulted in rapid urbanization of the area. Traditional Gibbs diagrams show some limitations because they are unable to identify the anthropogenic impacts on groundwater formation.

3.2 Contamination characteristics of heavy metals in groundwater

Descriptive statistics of the Cr, Ni, Zn, As, Cd, and Zn concentrations in dry and wet periods are listed in Table 1. The coefficient of variation (CV) values of the elements in the groundwater followed a descending order of Zn > Ni > Pb > As > Cr > Cd in the dry period and Zn > Ni > Cr > As > Pb > Cd in the wet period. Cr concentrations in the dry period were higher than in the wet period, and Zn concentrations in the dry period were lower than in the wet period, yet no significant changes were observed between the dry and wet periods in the other heavy metals. Concentrations of heavy metals varied significantly in the groundwater of this region. The CV values of Cr, As, Cd, and Pb were much lower than those of Zn and Ni in both periods. This indicates that the concentrations of Cr, As, Cd, and Pb were relatively less variable in each sampling site compared with those of Zn and Ni. This result leads us to speculate that concentrations of Zn and Ni in the groundwater have the highest probability of being influenced by extrinsic factors; that is, human activities (Lv et al., 2014). In addition, the CV values of Pb and Cd in the dry period were much lower than those in the wet period, implying that they may be subject to a significant seasonal impact (Hao et al., 2016).

The drinking groundwater standards of the US EPA, WHO, PCD of Thailand, and Chinese drinking water standards (GB 5749-2006) are shown in Table 2. The mean concentrations of As, Zn, Cd, and Pb in the dry period were

Table 2 Drinking groundwater standard

Heavy metals/(μg·L^{-1})	USEPA (2012)	PCD (2000)	WHO (2011)	GB 5749-2006 (2006)
Cr	100	50	50	50
Ni	*NA*	20	70	20
Zn	5000	5000	*NA*	1000
As	10	10	10	10
Cd	5	3	3	5
Pb	15	10	10	10

NA = not available.

(2.30±0.51, 12.28±21.76, 0.61±0.08, and 3.62±3.18) $\mu g \cdot L^{-1}$ and (3.36±0.48, 35.44±101.54, 1.01±0.01, and 7.66±0.32) $\mu g \cdot L^{-1}$ in the wet period (Table 1). By comparison, the heavy metal levels in groundwater were much higher in the wet period than the dry period. This indicated that As, Zn, Pb, and Cd might be leached from and desorbed by contaminated soils into shallow groundwater (Buchhamer et al., 2012). In addition, heavy metals could be leached out during the wet period due to the generally higher water table during this season. Similarly, more chemicals could be washed out directly from the vadose zone by infiltrating rainwater during the wet period (Hao et al., 2016).

In both the dry and wet periods, the concentrations of Cr, Zn, As, and Cd were lower than the Chinese drinking water standards (GB 5749-2006). However, the concentration of Ni in G11 (sampling depth 5 m, see Supporting Table 1) exceeded the standards in the two periods, whereas the concentration of Pb in G09 (sampling depth 16 m, see Supporting Table 1) exceeded the standards in the dry period. Moreover, G09 and G11 are located in areas of intensive agriculture and animal husbandry, which is usually accompanied by heavy pesticide use and the discharge of animal husbandry wastewater (Table 1; Fig. 1). The concentrations of Cr, Zn, Cd, and Pb in the groundwater sites were lower than the drinking water standards (except sites G09 and G11), suggesting that the water qualities were acceptable (Table 2).

3.3 The distribution and seasonal variation of heavy metals

The spatial distributions of heavy metals in groundwater were region-specific (Figs. 5–10). In the dry period, As, Cd, and Pb concentrations were low, showing homogeneous distributions across the study area, and indicating low natural background values. The highest concentrations of Cr and Ni were found at site G11, located close to a pig farm. Furthermore, another site with a high concentration of Cr was also located near a pig farm, indicating that the Cr and Ni are likely derived from animal husbandry wastewater.

The highest concentrations of Zn were found at G05,

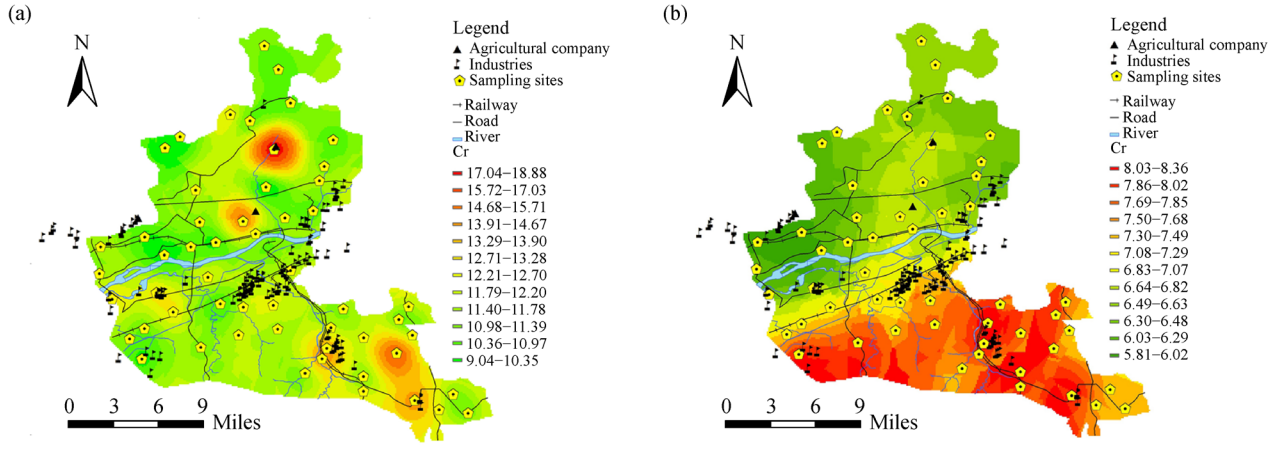

Fig. 5 Distribution of Cr in ground water in dry and wet periods. (a) Dry season; (b) wet season.

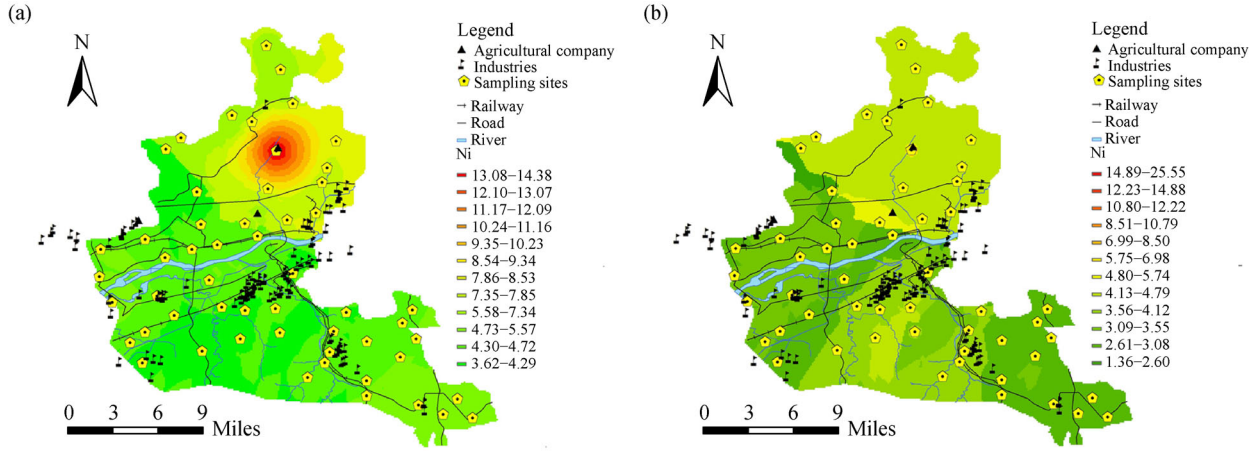

Fig. 6 Distribution of Ni in ground water in dry and wet periods. (a) Dry season; (b) wet season.

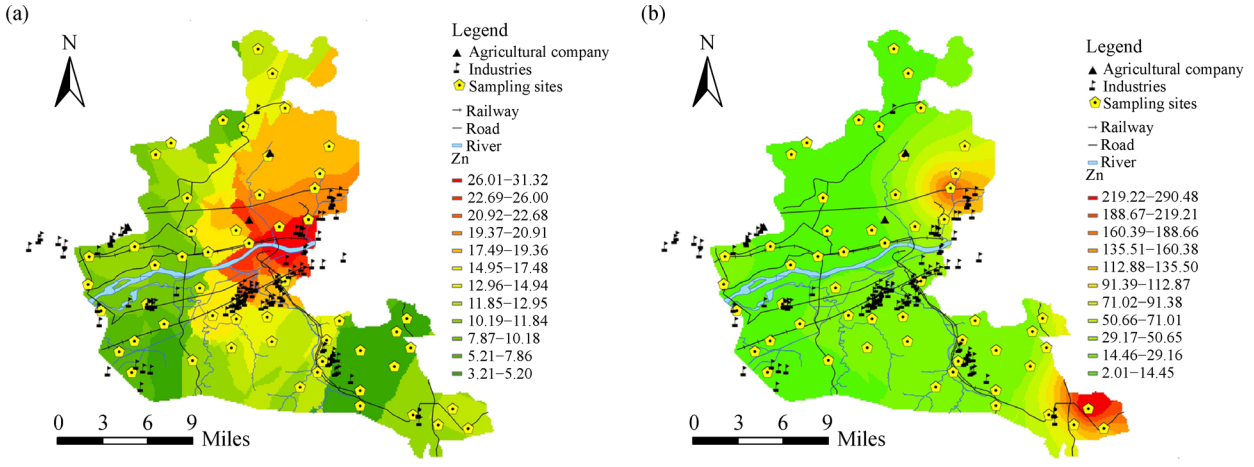

Fig. 7 Distribution of Zn in ground water in dry and wet periods. (a) Dry season; (b) wet season.

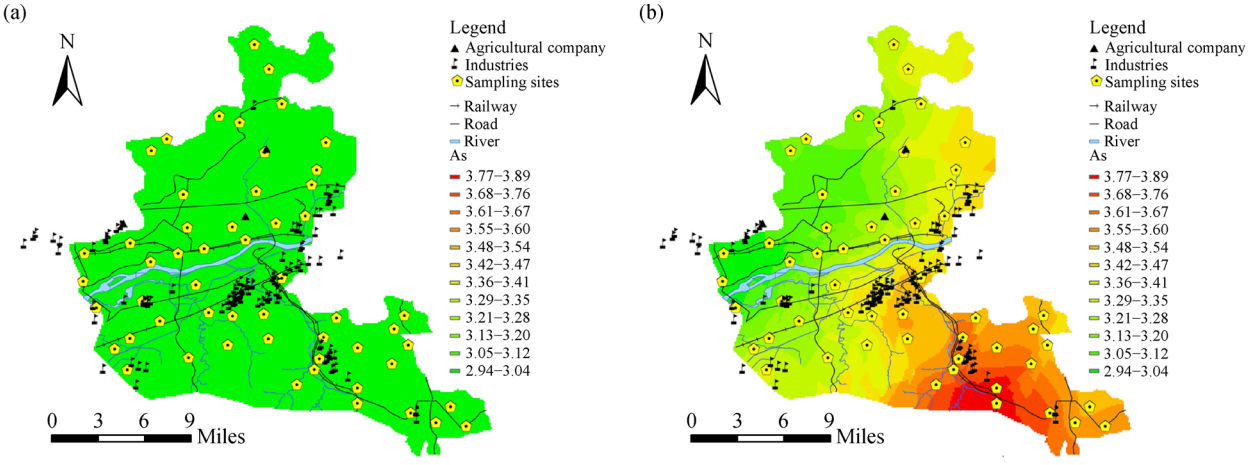

Fig. 8 Distribution of As in ground water in dry and wet periods. (a) Dry season; (b) wet season.

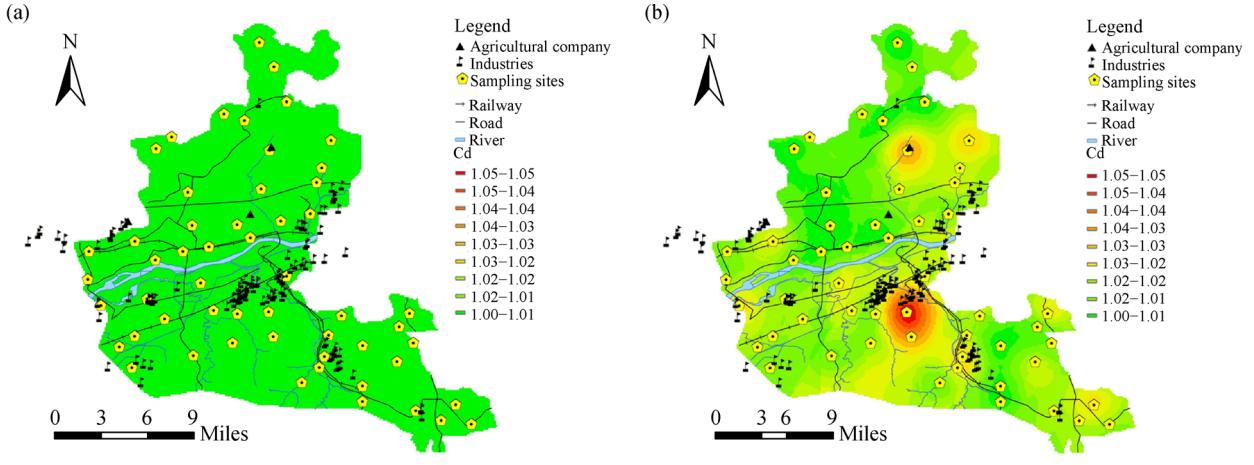

Fig. 9 Distribution of Cd in ground water in dry and wet periods. (a) Dry season; (b) wet season.

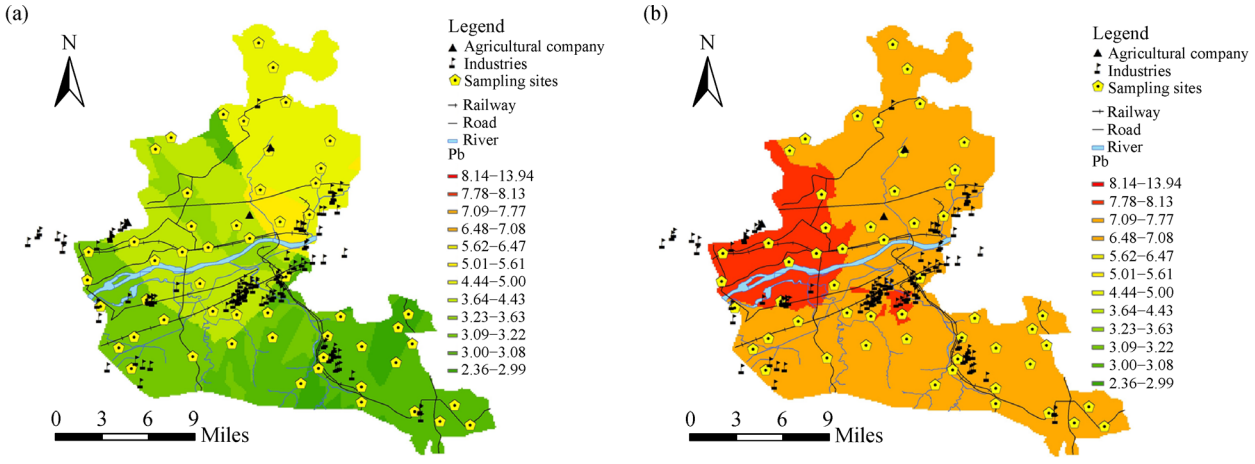

Fig. 10 Distribution of Pb in ground water in dry and wet periods. (a) Dry season; (b) wet season.

G06, G07, and G28, located in the vicinity of an urban area, suggesting that the Zn was primarily generated from industrial wastes, such as from foundry wastewater and instrument manufacturers (Hu et al., 2015). The groundwater was stagnant during the dry period, weakening the transport of the pollutants from upstream to downstream. The high values at some sites may have been due to high local inputs. For example, sites G30, G31, and G32 are located south of the Hun River near both petroleum and chemical companies as well as the Precision Instrument Foundry Company. The sampling depth in these sites was 5–10 m. It is presumed that the discharge of wastewater from urban runoff, nearby factories, and sewage outfalls in Fushun could be major sources. However, concentrations of As, Cd, Pb, and Zn were higher during the wet period than in the dry period. It is presumed that the difference in spatial distribution of the metals during the two periods was due to anthropogenic inputs, such as agricultural sources (Zhang et al., 2015b). However, the metals showed homogeneous distributions across the study area, except at some high value sites (such as As in G47 and G48, Cd in G11 and G30, Pb in G30, and Zn in G08 and G50), suggesting that As, Cd, Pb, and Zn were affected by human activities in these sites. Furthermore, the concentration of Cr in the south was higher than in the north (Fig. 5), and its high value sites were G35, G44, and G52, located near metal workshops, mechanical garages, and iron recycling shops. These observations are consistent with the results from Yolcubal et al. (2016). This study indicated that urbanizing development generated a high concentration of heavy metals. Anthropogenic activities associated with urban development generated pollutants and wastes on catchment surfaces that could be washed out to water bodies during storms (Barbosa et al., 2012). However, the distributions of Ni and Zn were similar in both periods, indicating that there were no new sources contributing to the two metals in the wet period.

3.4 Sources of the heavy metals in groundwater

Pearson's correlation coefficients were calculated for ions and related groundwater properties (ORP, EC, pH and salinity), as shown in Table 3. Measured pH values showed a negative correlation with Ca^{2+}, SO_4^{2-}, and Cl^- in the wet period. When the pH of water increases, aqueous metal species tend to precipitate as oxyhydroxide, hydroxide, or hydroxy-sulfate phases. Limestone and carbonate materials are two elements that can buffer pH changes in water.

A significant positive correlation ($P < 0.01$) was found between the elemental pairs Ni–Cr (0.62) in the dry period, which indicates that the two metals possibly had the same source. The concentration of Ni was relatively higher than the rest; and is an important by-product of some nearby factories, such as the foundries and electric control manufacturing companies. The concentration of Cr (Table 1) was much lower than the drinking groundwater standard (Table 2), and was moderately variable (the coefficient of variation is less than 36%), implying that Cr was not significantly affected by human activities. Moreover, Ni and Cr were not found to have a significant positive correlation during the wet period (Table 3), suggesting that the inputs from agricultural production are affected by seasonal changes, which disturbed the original correlation of Ni and Cr. Furthermore, a negative correlation of metals in the dry period was found between the elemental pairs Cd-Ni (–0.40) and Cd-Cr (–0.56), indicating that the sources of Cd are different from those of Cr and Ni. However, in the wet period, As-Cr (0.46) and Cd-Ni (0.48) had a significant positive correlation. It is reasonable to assume that the concentration distribution of Cd and As could be affected by both natural processes (Wu et al., 2015) and human activities (such as agricultural sources).

In addition, the concentrations of Pb and Zn showed relatively poor correlations with other metals. This could

Table 3 Pearson's correlation matrix for the concentrations of heavy metals and groundwater properties

		Cr	Ni	Zn	As	Cd	Pb	Ca^{2+}	Mg^{2+}	SO_4^{2-}	Cl^-	ORP	EC	pH	SAL
Dry Period	Cr	1													
	Ni	0.62**	1												
	Zn	–0.03	0.08	1											
	As	–0.01	0.01	0.01	1										
	Cd	–0.56**	–0.40**	0.05	0.13	1									
	Pb	–0.08	0.01	–0.05	–0.08	0.08	1								
	Ca^{2+}	–0.16	–0.11	0.11	–0.10	0.07	–0.10	1							
	Mg^{2+}	0.09	0.10	0.00	–0.12	0.01	0.25	0.43**	1						
	SO_4^{2-}	0.00	0.07	0.15	0.11	–0.07	0.10	–0.01	0.05	1					
	Cl^-	–0.02	0.12	0.09	0.02	–0.01	0.08	0.03	0.12	0.82**	1				
	ORP	0.04	0.28*	0.14	–0.26	0.01	0.19	0.14	0.29*	0.11	0.18	1			
	EC	0.09	0.41**	–0.06	0.31*	–0.04	–0.07	–0.03	0.02	0.04	0.02	0.30*	1		
	pH	0.00	–0.07	–0.18	0.23	–0.11	–0.12	–0.18	–0.26	–0.19	–0.20	–0.91**	–0.26	1	
	SAL	0.12	0.43**	0.24	0.35*	–0.02	–0.07	0.06	–0.03	0.13	0.08	0.43**	0.86**	–0.42**	1
Wet Period	Cr	1													
	Ni	–0.02	1												
	Zn	–0.07	–0.03	1											
	As	0.45**	0.23	–0.01	1										
	Cd	0.06	0.47**	0.21	0.14	1									
	Pb	0.10	0.03	–0.06	0.02	0.29*	1								
	Ca^{2+}	–0.20	0.39**	–0.13	0.08	0.50**	0.13	1							
	Mg^{2+}	–0.38**	0.35*	–0.16	–0.07	0.28*	0.04	0.75**	1						
	SO_4^{2-}	–0.05	0.10	–0.05	0.10	0.17	0.00	0.18	0.06	1					
	Cl^-	–0.03	0.35*	–0.08	0.20	0.30*	0.13	0.36**	0.18	0.88**	1				
	ORP	0.01	0.20	0.02	0.04	0.26	–0.04	0.47**	0.15	0.46**	0.45**	1			
	EC	–0.32*	0.53**	–0.10	0.06	0.50**	0.08	0.82**	0.81**	0.25	0.40**	0.34*	1		
	pH	–0.05	–0.19	–0.05	–0.05	–0.27	0.05	–0.48**	–0.21	–0.38**	–0.40**	–0.94**	–0.33*	1	
	SAL	–0.32*	0.53**	–0.10	0.07	0.50**	0.07	0.82**	0.81**	0.24	0.39**	0.33*	0.99**	–0.33*	1

** Correlation is significant at the 0.01 level (2-tailed). * Correlation is significant at the 0.05 level (2-tailed).

be attributed to natural and anthropogenic source inputs for these elements, which disturbed the original correlation. Some water samples, such as from site G30, contained relatively high Pb (Fig. 1, Table 1, and Table 2). The concentrations of other elements (such as Cd, Cr, and As) were low. Given unleaded petrol was first used in Shenfu New District many years ago, contamination from storm-water from transportation routes is unlikely. There are some lead-zinc mines near Fusun City, such as galena, anglesite, cerussite, and sphalerite. Pb can be found naturally in anglesite (lead sulfate, $PbSO_4$), galena (lead sulfide, PbS), minim (a form of lead oxide with the formula Pb_3O_4), cerussite (lead carbonate, $PbCO_3$), and other minerals. When there is CO_2 in the groundwater and porous rocks, galena may be the most important natural source (Li et al., 2008). As for solubility trapping, CO_2 dissolves and becomes miscible in groundwater. It then migrates through dispersion, diffusion, and convection with the aquifer's regional hydrodynamic regime. In the end, CO_2-water-rock reactions can lead to mineral dispersion into the groundwater (Smedley and Kinniburgh, 2002; Farquhar et al., 2015). Therefore, the distribution of heavy metals can become modified by natural processes; such as through water-rock interactions. Thus, when considering the previous conclusion, these trace elements may be the result of both anthropogenic pollution and natural processes.

To identify clusters of metals, hierarchical cluster analysis (HCA) was performed on the dataset of variables (Fig. 11). The results of the dry period enabled the identification of three main groups to describe the complex reality of the area studied, which were designated A (As, Cd, and Pb), B (Cr and Ni), and C (Zn). The results of cluster analysis and correlation analysis were in agreement,

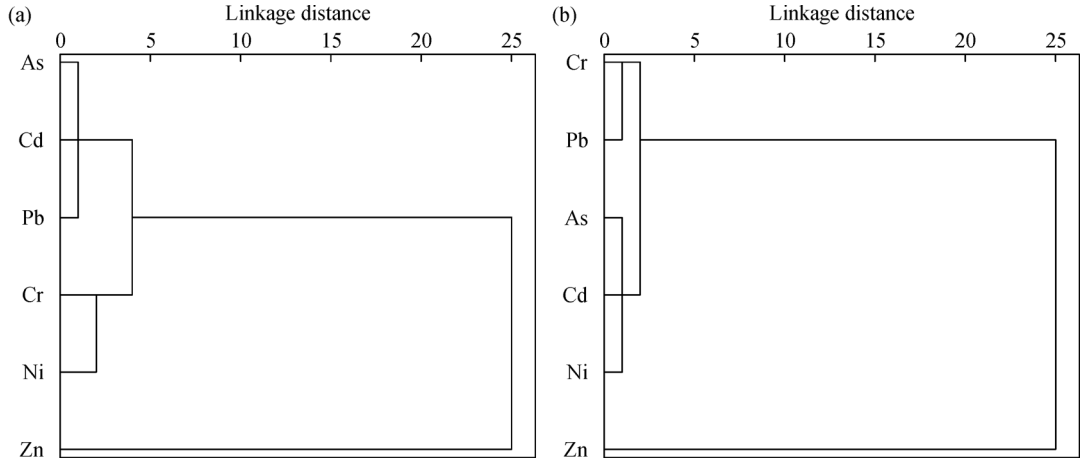

Fig. 11 Tree diagram for six variables of ground water both in dry and wet periods. (a) Dry season; (b) wet season.

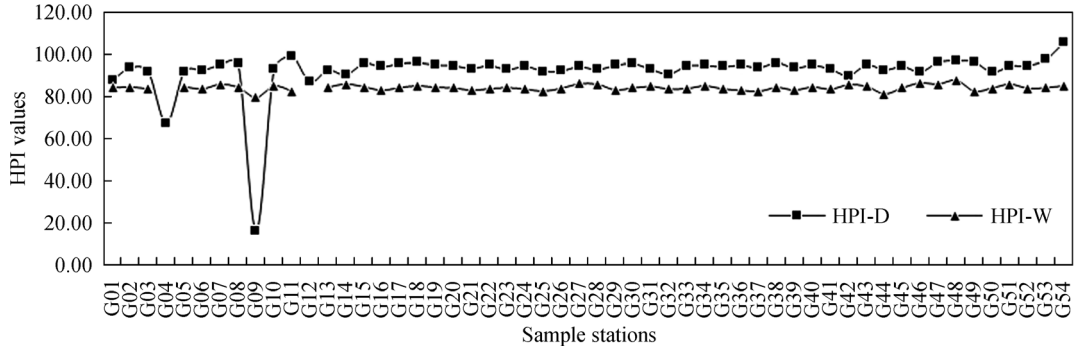

Fig. 12 Spatial distribution of the heavy metal pollution index.

indicating that the above conclusion on metal sources is credible. However, the dendrogram of metals in the wet period displayed three different clusters. In the first cluster, Pb and Cr were well associated with each other. The second cluster was comprised of As, but was also linked with Cd and Ni. In the third cluster, there was only Zn. Differences in the results of HCA during the wet period and the dry period could be due to changes in natural conditions (such as rainfall infiltration and stream recharge), which disturbed the original correlation.

3.5 Pollution assessment index and potential ecosystem risk assessment

To calculate the HPI of the groundwater in Shenfu New District, the concentrations of Cr, Ni, Zn, As, Cd, and Zn in both dry and wet periods were considered. Table 4 shows the detailed results of HPI with standard permissible values (S_i) and unit weighting (W_i) for dry and wet periods at 91.85 and 70.87, respectively, below the critical value of 100. These results indicate that, in general, the groundwater was not critically contaminated by heavy metals. The HPI of each sampling point was calculated separately (see Table 5), and the metal pollution index of each sampling site was also determined. The HPI values indicated similar trends at different sampling sites (Fig. 12), with only site G54 above the critical value of 100.

The potential ecological risk of heavy metals was analyzed based on the data collection and analysis. Concentrations of Pb in groundwater exceeding 10 $\mu g \cdot L^{-1}$ imply heavy contamination. Additionally, a concentration of Ni in groundwater exceeding 20 $\mu g \cdot L^{-1}$ implies that it is unfit for human consumption. Even though heavy metals do not show highly acute toxicity to human beings, Ni and Pb did tend to exhibit higher levels in some sites; for example, the concentrations of Pb in sites G10 and G05, and Ni in site G12 exceeded safety values. In comparison with other groundwater systems around the world, the mean concentrations of heavy metals in the Shenfu New District were lower than those of Yaoundé, Cameroon, but significantly higher than those of Berkshire, UK (Table 5). In addition, the mean concentrations of Cr and Cd in the Shenfu New District were much higher than those in Hong Kong, China and Ubon Ratchathani, Thailand. Similarly, the concentrations of Ni and Pb in Shenfu New District were slightly higher than those in the Yellow River region (Zhang et al., 2015b).

For individual heavy metals, Zn was the most commonly

Table 4 HPI calculations for ground water of Shenfu New District

Metals	M_i^D	M_i^W	S_i	I_i	Unit Weightage (W_i)	Sub-index (Q_i^D)	Sub-index (Q_i^W)	$W_iQ_i^D$	$W_iQ_i^W$
Cr	11.64	7.03	100	50	0.010	76.72	85.94	0.7672	0.8594
Ni	5.29	3.40	70	20	0.014	29.42	33.20	0.4119	0.4648
Zn	12.28	35.44	5000	1000	0.0002	24.69	24.11	0.0049	0.0048
As	2.30	3.36	10	-	0.100	23.00	33.60	2.3000	3.3600
Cd	0.61	1.01	5	3	0.200	119.50	99.50	23.9000	19.9000
Pb	3.62	7.66	15	10	0.067	127.60	46.80	8.5492	3.1356

M_i = concentration, S_i = standard value, I_i = ideal value, W = wet season, D = dry season. $\sum W_i = 0.3912$, $\sum W_iQ_i^D = 35.93$, $HPI^D = 91.85$; $\sum W_iQ_i^W = 27.72$, $HPI^W = 70.87$.

Table 5 Concentration ranges and mean values of heavy metals in groundwater from different areas

Site	Cr/(μg·L^{-1})		Ni/(μg·L^{-1})		Zn/(μg·L^{-1})		As/(μg·L^{-1})		Cd/(μg·L^{-1})		Pb/(μg·L^{-1})		References
	Range	Mean	Range	Mean	Range	Mean	Range	Mean	Range	Mean	Range	Mean	
Hong Kong, China	0.60–5.12	1.12	NA	NA	7.39–92.39	40.83	0.12–17.49	2.65	0.01–1.18	0.14	0.03–6.67	0.74	Leung Jiao (2006)
Ubon Ratchathani, Thailand	0.29–2.14	0.58	1.34–15.6	6.13	6.94–302	63.4	0.25–6.44	1.06	0.13–0.23	0.15	0.95–66.90	16.7	Wongsasuluk et al. (2014)
Berkshire, UK	< 1.00	< 1.00	2.00–11.00	3.00	1.30–34.00	9.90	1.00–4.00	2.00	< 2.00	< 2.00	2.00–10.00	6.40	Edmunds et al. (2003)
Yaoundé	640–1330	920	250–630	440	NA	NA	NA	NA	0–80	27.50	280–340	307.50	Defo et al. (2015)
Yellow River	NA	NA	0–26.00	4.00	5.00–61400	7400	NA	NA	NA	NA	0–10.00	3.00	Sun et al. (2017)
Shenfu New District	4.73–21.15	9.32	1.03–47.94	4.35	0.71–607.40	24.15	1.09–4.66	2.83	0.17–1.07	0.81	1.98–25.46	5.64	This study

NA = not available.

detected heavy metal in drinking water. Its presence under normal conditions, however, did not pose a hazard to human health. Our results showed that the concentrations of the heavy metals varied under different climatic conditions and human activities in different areas. The levels of heavy metals in groundwater near the Hun River were relatively high. This is because the sampling sites were located in the heavy industrial areas of Northeast China.

4 Conclusions

The seasonal and spatial variations and risk assessment of Cr, Ni, Zn, As, Cd, and Pb were investigated in groundwater. The hydrogeochemical properties of groundwater can be affected by neutral and slightly acidic pH and low EC. In addition, the concentrations of Ni, Cr, Zn, Cd, As, and Pb in the groundwater indicated great seasonal variation. The mean concentrations of Zn, As, Pb, and Cd in the wet period were about twice those of the dry period. These elements might be desorbed by and leached from contaminated soils into shallow groundwater. The spatial distributions of the heavy metals in groundwater were region-specific. The highest concentrations of heavy metals were mostly found along the Hun River. This was due to the location of the sampling sites in a heavy industrial area of Northeast China. Ni and Cr concentrations indicate the same anthropogenic origin (i.e., wastewater from agricultural product processing). Concentrations of Zn are high under natural conditions, and are also affected by human activities (e.g., waste water from foundry and instrument manufacturers). As, Cd, and Pb were likely affected by both anthropogenic and natural sources (e.g., agricultural sources and water-rock interactions). The HPI values in wet and dry periods showed similar trends, with the critical value over 100 observed in site G54. Even though the ecological risk is currently low in the Shenfu New District, there is a potential for toxic effects in the future. This information could be used for the development of effective management strategies to reduce air pollution in the Shenfu New District.

Acknowledgements The authors wish to thank the Water Foundations of China (2014ZX07202-011). The authors also appreciate support from the Beijing Key Laboratory of Aqueous Typical Pollutants Control and Water

Quality Safeguard. We also thank LetPub (www.letpub.com) for its linguistic assistance during the preparation of this manuscript.

References

Al-Omran A M, Aly A A, Al-Wabel M I, Sallam A S, Al-Shayaa M S (2016). Hydrochemical characterization of groundwater under agricultural land in arid environment: a case study of Al-Kharj, Saudi Arabia. Arab J Geosci, 9(1): 1–17

Barbosa A E, Fernandes J N, David L M (2012). Key issues for sustainable urban stormwater management. Water Res, 46(20): 6787–6798

Baumann T, Fruhstorfer P, Klein T, Niessner R (2006). Colloid and heavy metal transport at landfill sites in direct contact with groundwater. Water Res, 40(14): 2776–2786

Borrell A, Tornero V, Bhattacharjee D, Aguilar A (2016). Trace element accumulation and trophic relationships in aquatic organisms of the Sundarbans mangrove ecosystem (Bangladesh). Sci Total Environ, 545–546: 414–423

Buchhamer E E, Blanes P S, Osicka R M, Giménez M C (2012). Environmental risk assessment of arsenic and fluoride in the Chaco Province, Argentina: research advances. J Toxicol Environ Health, 75 (22–23): 1437–1450

Cui J, Du J Z, Wang X G (2014). Contamination characteristics in surface water and coastal ground water of Hunhe River. Acta Ecol Sin, 34(7): 1860–1869 (in Chinese)

Cui L, Shi J (2012). Urbanization and its environmental effects in Shanghai, China. Urban Climate, 2: 1–15

De Nicola F, Baldantoni D, Sessa L, Monaci F, Bargagli R, Alfani A (2015). Distribution of heavy metals and polycyclic aromatic hydrocarbons in holm oak plant–soil system evaluated along urbanization gradients. Chemosphere, 134: 91–97

Defo C, Yerima B P, Noumsi I M, Bemmo N (2015). Assessment of heavy metals in soils and groundwater in an urban watershed of Yaoundé (Cameroon-west Africa). Environmental Monitoring & Assessment, 187(3): 77–85

Dokou Z, Kourgialas N N, Karatzas G P (2015). Assessing groundwater quality in Greece based on spatial and temporal analysis. Environ Monit Assess, 187: 774

Edmunds W M, Shand P, Hart P, Ward R S (2003). The natural baseline quality of ground water: a UK pilot study. Sci Total Environ, 2003, 310(1–3): 25–35

Erbahar D D, Gumus G, Pamir O, Musluoglu E, Ahsen V, Gurol L, Harbeck M (2016). Polyalkoxy substituted phthalocyanines sensitive to phenolic compounds in water. Sens Actuators B Chem, 227: 277–282

Farquhar S M, Pearce J K, Dawson G K W, Golab A, Sommacal S, Kirste D, Biddle D, Golding S D (2015). A fresh approach to investigating CO_2 storage: experimental CO_2–water–rock interactions in a low-salinity reservoir system. Chem Geol, 399: 98–122

Gao X, Zhang Y, Ding S, Zhao R, Meng W (2015). Response of fish communities to environmental changes in an agriculturally dominated watershed (Liao River Basin) in northeastern China. Ecol Eng, 76: 130–141

Gibbs R J (1970). Mechanisms Controlling World Water Chemistry. Science, 170: 1088–1090

Guo R, He X (2013). Spatial variations and ecological risk assessment of heavy metals in surface sediments on the upper reaches of Hun River, Northeast China. Environ Earth Sci, 70(3): 1083–1090

Guo W, He M C, Yang Z F, Lin C Y, Quan X C (2010). Occurrence of aliphatic hydrocarbons in water, suspended particulate matter and sediments of Daliao River system, China. Bull Environ Contam Toxicol, 84(5): 519–523

Hao X, Wang D, Wang P, Wang Y, Zhou D (2016). Evaluation of water quality in surface water and shallow groundwater: a case study of a rare earth mining area in southern Jiangxi Province, China. Environ Monit Assess, 188(1): 1–11

Hosseinifard S J, Aminiyan M M (2015). Hydrochemical characterization of groundwater quality for drinking and agricultural purposes: a case study in Rafsanjan plain, Iran. Water Qual Expo Health, 7(4): 531–544

Hu G, Bi S, Xu G, Zhang Y, Mei X, Li A (2015). Distribution and assessment of heavy metals off the Changjiang River mouth and adjacent area during the past century and the relationship of the heavy metals with anthropogenic activity. Mar Pollut Bull, 96(1–2): 434–440

Kujawska J, Pawlowska M, Cel W, Pawlowski A (2016). Potential influence of drill cuttings landfill on groundwater quality-comparison of leaching tests results and groundwater composition. Desalination Water Treat, 57(3): 1409–1419

Li F D, Pan G, Tang C, Zhang Q, Yu J (2008). Recharge source and hydrogeochemical evolution of shallow groundwater in a complex alluvial fan system, southwest of North China Plain. Environmental Geology, 55(5): 1109–1122

Li P, Qian H, Howard K W F, Wu J (2015). Building a new and sustainable “Silk Road economic belt”. Environ Earth Sci, 74(10): 7267–7270

Li P, Tian R, Xue C, Wu J (2017). Progress, opportunities and key fields for groundwater quality research under the impacts of human activities in China with a special focus on western China. Environ Sci Pollut Res Int, 24(15): 13224–13234

Li P, Wu J, Qian H (2016b). Hydrochemical appraisal of groundwater quality for drinking and irrigation purposes and the major influencing factors: a case study in and around Hua County, China. Arab J Geosci, 9(1): 1–17

Li P, Wu J, Qian H, Zhang Y, Yang N, Jing L, Yu P (2016a). Hydrogeochemical characterization of groundwater in and around a wastewater irrigated forest in the southeastern edge of the Tengger Desert, Northwest China. Expo Health, 8(3): 331–348

Leung C M, Jiao J J (2006). Heavy metal and trace element distributions in groundwater in natural slopes and highly urbanized spaces in Mid-Levels area, Hong Kong. Water Research, 40(4): 753–767

Lv J, Liu Y, Zhang Z, Dai B (2014). Multivariate geostatistical analyses of heavy metals in soils: spatial multi-scale variations in Wulian, Eastern China. Ecotox environ safe, 107: 140–147

Long M, Wu J, Abuduwaili J (2016). Hydrochemical and isotopic characters of surface water in agricultural oases of the Tianshan Mountains, Northwest China. Arid Land Res Manage, 30(1): 37–48

Mehrabi B, Mehrabani S, Rafiei B, Yaghoubi B (2015). Assessment of metal contamination in groundwater and soils in the Ahangaran mining district, west of Iran. Environ Monit Assess, 187(12): 727

Nwaichi E O, Wegwu M O, Nwosu U L (2014). Distribution of selected carcinogenic hydrocarbon and heavy metals in an oil-polluted agriculture zone. Environ Monit Assess, 186(12): 8697–8706

Peng C, Wang M, Zhao Y, Chen W (2016). Distribution and risks of polycyclic aromatic hydrocarbons in suburban and rural soils of Beijing with various land uses. Environ Monit Assess, 188(3): 1–12

Peng J, Ren Z, Song Y, Yu H, Tang X, Gao H (2015). Impact of spring flooding on DOM characterization in a small watershed of the Hun River, China. Environ Earth Sci, 73(9): 5131–5140

Piper A M (1944). A graphical interpretation of water-analysis. Trans Am Geophys Union, 25: 914–928

Prasad B, Jaiprakas K C (1999). Evaluation of heavy metals in ground water near mining area and development of heavy metal pollution index. J Environ Sci Health, 34: 91–102

Prasad B, Sangita K (2008). Heavy metal pollution index of ground water of an abandoned open cast mine filled with fly ash: a case study. Mine Water Environ, 27(4): 265–267

Rasool A, Farooqi A, Masood S, Hussain K (2016). Arsenic in groundwater and its health risk assessment in drinking water of Mailsi, Punjab, Pakistan. Hum Ecol Risk Assess, 22(1): 187–202

Rodríguez J A, Nanos N, Grau J M, Gil L, López-Arias M (2008). Multiscale analysis of heavy metal contents in Spanish agricultural topsoils. Chemosphere, 70(6): 1085–1096

Siegel D I, Smith B, Perry E, Bothun R, Hollingsworth M (2015). Pre-drilling water-quality data of groundwater prior to shale gas drilling in the Appalachian Basin: analysis of the Chesapeake Energy Corporation dataset. Appl Geochem, 63: 37–57

Smedley P L, Kinniburgh D G (2002). A review of the source, behaviour and distribution of arsenic in natural water. Appl Geochem, 17(5): 517–568

Strugała-Wilczek A, Stańczyk K (2016). Leaching behaviour of metals from post-underground coal gasification cavity residues in water differing in mineralization. Fuel, 173: 106–114

Su X, Yuan W, Xu W, Du S (2015). A groundwater vulnerability assessment method for organic pollution: a validation case in the Hun River basin, Northeastern China. Environ Earth Sci, 73(1): 467–480

Sun H, Li F, Zhang T, Zhang X, He N, Song Q, Zhao L, Sun L, Sun T (2011). Perfluorinated compounds in surface waters and WWTPs in Shenyang, China: mass flows and source analysis. Water Res, 45(15): 4483–4490

Sun Z, Mou X, Zhang D, Sun W, Hu X, Tian L (2017). Impacts of burial by sediment on decomposition and heavy metal concentrations of suaeda salsa in intertidal zone of the Yellow River estuary, China. Mar Pollut Bull, 116(1–2): 103–112

Wang J, Liu G, Lu L, Zhang J, Liu H (2015). Geochemical normalization and assessment of heavy metals (Cu, Pb, Zn, and Ni) in sediments from the Huaihe River, Anhui, China. Catena, 129: 30–38

Wang Y, Jiao J J (2012). Origin of groundwater salinity and hydrogeochemical processes in the confined Quaternary aquifer of the Pearl River Delta, China. J Hydrol (Amst), 438–439: 112–124

Wang Z, Lin C, He M, Quan X, Yang Z (2010). Phosphorus content and fractionation of phosphate in the surface sediments of the Daliao river system in China. Environ Earth Sci, 59(6): 1349–1357

Wongsasuluk P, Chotpantarat S, Siriwong W, Robson M (2014). Heavy metal contamination and human health risk assessment in drinking water from shallow groundwater wells in an agricultural area in Ubon Ratchathani province. Environ Geochem Hlth, 36(1): 169–182

Wu J, Li P, Qian H (2015). Hydrochemical characterization of drinking groundwater with special reference to fluoride in an arid area of China and the control of aquifer leakage on its concentrations. Environ Earth Sci, 73(12): 8575–8588

Wu J, Li P, Qian H, Duan Z, Zhang X (2014). Using correlation and multivariate statistical analysis to identify hydrogeochemical processes affecting the major ion chemistry of waters: case study in Laoheba phosphorite mine in Sichuan, China. Arab J Geosci, 7(10): 3973–3982

Wuana R A, Okieimen F E (2011). Heavy metals in contaminated soils: a review of sources, chemistry, risks and best available strategies for remediation. ISRN Ecol, 2011: 1–20

Xu B, Xu Q, Liang C, Li L, Jiang L (2015). Occurrence and health risk assessment of trace heavy metals via groundwater in Shizhuyuan Polymetallic Mine in Chenzhou City, China. Front Environ Sci Eng, 9(3): 482–493

Yao J, He X Y, Li X Y, Chen W, Tao D L (2012). Monitoring responses of forest to climate variations by MODIS NDVI: a case study of Hun River upstream, northeastern China. Eur J For Res, 131(3): 705–716

Yolcubal I, Gunduz O C, Sonmez F (2016). Assessment of impact of environmental pollution on groundwater and surface water qualities in a heavily industrialized district of Kocaeli (Dilovasi), Turkey. Environ Earth Sci, 75(2): 1–23

Zhang H, Sun L, Sun T, Li H, Luo Q (2013). Spatial distribution and seasonal variation of polycyclic aromatic hydrocarbons (PAHs) contaminations in surface water from the Hun River, Northeast China. Environ Monit Assess, 185(2): 1451–1462

Zhang L, Shi Z, Zhang J, Jiang Z, Wang F, Huang X (2015a). Spatial and seasonal characteristics of dissolved heavy metals in the east and west Guangdong coastal waters, South China. Mar Pollut Bull, 95(1): 419–426

Zhang Y, Guo F, Meng W, Wang X (2009). Water quality assessment and source identification of Daliao river basin using multivariate statistical methods. Environ Monit Assess, 152(1–4): 105–121

Zhang Y, Li F, Li J, Liu Q, Tu C, Suzuki Y, Huang C (2015b). Spatial distribution, potential sources, and risk assessment of trace metals of groundwater in the North China Plain. Hum Ecol Risk Assess, 21(3): 726–743

Zou J, Dai W, Gong S, Ma Z (2015). Analysis of spatial variations and sources of heavy metals in farmland soils of Beijing Suburbs. PLoS One, 10(2): e0118082